Journal of Physics: Conference Series

PAPER • **OPEN ACCESS**

Study on Fracture Parameters of Stress Corrosion Cracking Tip of AA6082 Alloy at the Microscopic Scale

To cite this article: Jia Song *et al* 2021 *J. Phys.: Conf. Ser.* **2002** 012001

View the article online for updates and enhancements.

This content was downloaded from IP address 116.49.38.244 on 30/08/2021 at 02:48

Study on Fracture Parameters of Stress Corrosion Cracking Tip of AA6082 Alloy at the Microscopic Scale

Jia Song[1], Ding Fan[1], Wenheng Wu[1], Liming Lei[2], Liang Zhang[1*] and Zhibin Gao[3*]

[1] Shanghai Engineering Research Center of 3D Printing Materials, Shanghai Research Institute of Materials, Shanghai 200437, China
[2] AECC Commercial Aircraft Engine Co., LTD, Shanghai 201104, China
[3] Department of Physics, National University of Singapore, Singapore 117551, Republic of Singapore
E-mail: lzhang0126@hotmail.com (Liang Zhang); zhibin.gao@xjtu.edu.cn (Zhibin Gao)

Abstract. A two-dimensional finite element model is used to explore the fracture parameter in the tip region of stress corrosion crack (SCC) of AA6082 alloy. Based on the ABAQUS code, we investigate the effect of oxide film's yield stress on the Mises stress and equivalent plastic strain (PEEQ) in the crack tip. The results show that as the yield strength of oxide film increases, the Mises stress and PEEQ of base alloy in crack tip area both decrease, and the stress of oxide film in crack tip also reduces, but the strain increases. This is because the oxide film bears more load, so the load on the base alloy of the crack tip becomes smaller, resulting in a reduction in the stress and strain on the base.
Keywords: AA6082 alloy, Stress corrsion crack, Finite element modelling

1. Introduction

In recent year, aluminum alloy has aroused great public attention because of its high specific strength, high specific stiffness, and excellent heat resistance. The alloy has the potential to replace some Ti alloys applied in aviation and aerospace industries [1-4]. Among them, AA6082 (Al-Si-Mg-Mn) is the most attractive because it combines fine weldability, corrosion resistance, formability, and machinability [5]. In the high-temperature water, however, the stress corrosion crack (SCC) of AA6082 alloy may affect the safe operation and service of the device, and the experimental characterization of the stress-strain field at the crack tip is exceedingly difficult, which severely limits the understanding of stress corrosion mechanisms and influencing factors.

With the development of computer technology, studying the environment, materials, and mechanical atmosphere of the stress corrosion sensitivity tip fracture process area by multi-scale modeling has become one of the important tools to deeply understand the mechanism and propagation rate of SCC [6-9]. In this work, a two-dimensional oxide film model is proposed to simulate related fracture parameters in a tip area of SCC of AA6082 alloy under three different yield stresses of oxide film. The finite element analysis is performed with ABAQUS code and the two-dimensional model is composed of matrix alloy and oxide film.

Content from this work may be used under the terms of the Creative Commons Attribution 3.0 licence. Any further distribution of this work must maintain attribution to the author(s) and the title of the work, journal citation and DOI.
Published under licence by IOP Publishing Ltd

2. Finite Element Modeling Method

2.1. Geometrical Model

In the high-temperature water, AA6082 alloy reacts with the medium to form a dense oxide film with a thickness of 1~2 μm on the alloy surface, thus, the thickness of oxide film in this research is 1.5 μm [10]. The two-dimensional model size is 100×100 μm^2, as shown in figure 1a, in which the grey area is the matrix alloy (AA6082 alloy), and the blue area is the oxide film formed on the alloy surface. Meanwhile, to better understand the fracture atmosphere of the crack tip and facilitate subsequent analysis, the tip area is described in detail, as shown in figure 1b, the three observation lines are used to analyze the stress-strain value in the tip area of SCC. Observation line 1 is located in the matrix alloy, 0.5 μm away from the interface between the oxide film and the matrix alloy, observation line 2 is located in the oxide film, 0.5 μm away from the interface between the oxide film and the matrix alloy, and observation line 3 follows the direction of crack propagation. With the three observation lines, the distribution of stress and strain in the matrix alloy, oxide film and along the crack propagation direction are studied.

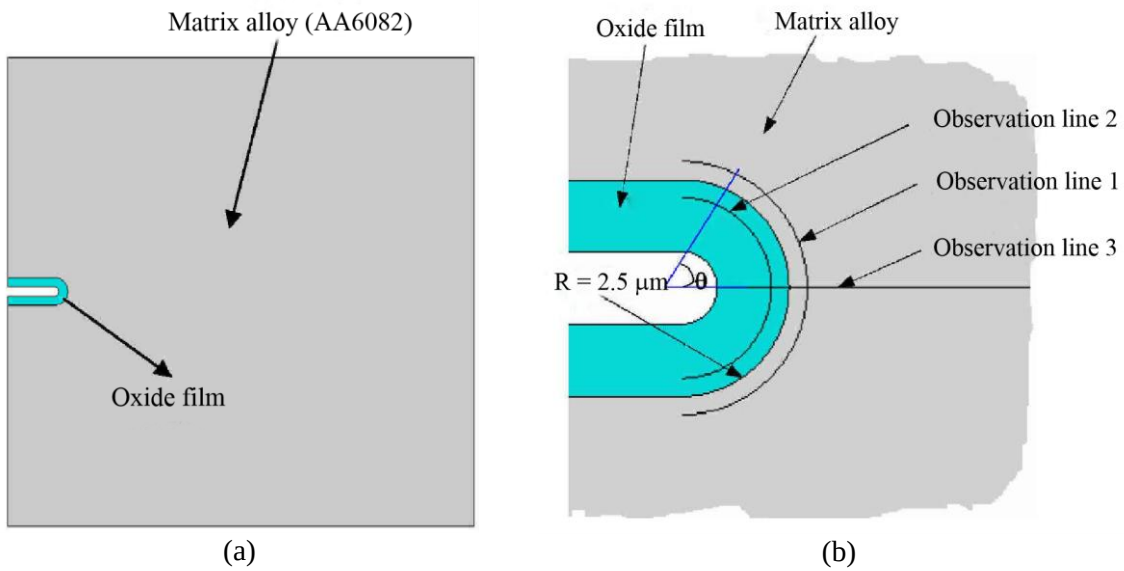

Figure 1. The two-dimensional model (a) and the detail of the crack tip region (b).

2.2. Material Model

The definition of materials is a particularly important part in numerical simulation, which will directly affect the accuracy and reliability of numerical simulation results. Therefore, in the numerical simulation analysis, the constitutive relationship between matrix aluminum alloy and the oxide film material in the crack tip region is assumed to be Ramberg-Osgood function [11]

$$\frac{\varepsilon}{\varepsilon_0}=\frac{\sigma}{\sigma_0}+\alpha\left(\frac{\sigma}{\sigma_0}\right)^n$$

in which, α is deviation coefficient, n is hardening exponent, and σ, ε, σ_0, and ε_0 are true stress, true strain, yield stress and, and yield strain, respectively.

The material parameters of matrix alloy and oxide film in the model are elastic modulus (E), Poisson's ratio (v), yield stress (σ_0), deviation coefficient (α), and hardening exponent (n). In this study, the α and n of matrix alloy and oxide film are the same and set as 1 and 5.29, respectively. The E and ε_0 of oxide film are considered to be one tenth of those of the matrix alloy. The mechanical parameters of base alloy and oxide film are list in table 1.

Table 1. Mechanical parameters of base alloy and oxide film.

Materials	Elastic modulus (E) MPa	Poisson's ratio (v)	Yield stress (σ_0) MPa
Oxide film	7089.9	0.33	17.6
	7089.9	0.33	22.0
	7089.9	0.33	26.4
AA6082 alloy	70899	0.33	220

2.3. Mesh Model

Figure 2a displays the mesh of the two-dimensional model. The mesh adopts an 8-node quadratic plane strain quadrilateral element (CPE8), and the total number of model elements is 48994. Due to the large stress gradient at the interface between the oxide film and the matrix alloy, the oxide film and matrix alloy in the crack tip area are finely meshed to obtain more detailed and accurate stress and strain data of the crack tip, as shown in figure 2b. The cell near the interface is about 0.067 μm, with good mesh transition and no distortion.

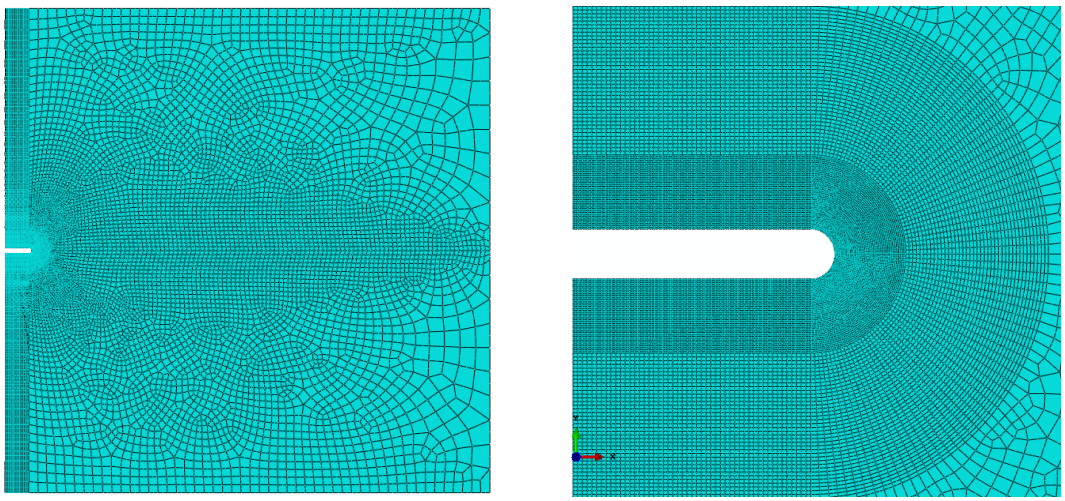

(a) (b)

Figure 2. The mesh of the two-dimensional model (a) and the detail mesh of the crack tip region (b).

3. Results and Discussions

3.1. Influence of Oxide Film's Yield Stress on the Stress and Strain Along Line 1

Figure 3 is the Mises stress and equivalent plastic strain curve of the base alloy in the crack tip when the yield strength of oxide film material is different. From figure 3a, it can be seen that the increase of the oxide film material's yield stress reduces the Mises stress of the base alloy in the crack tip area and the maximum stress is at θ=0 °. When the θ varies from -30 °to 30 °, the Mises stress changes little, from 125 MPa to 135 MPa, the absolute value of θ is between the 70 °and 30 °, the Mises stress changes greatly, from 105 MPa to 120 MPa, and the absolute value of θ is in the range of 70 °~90 °, the Mises stress changes the most, from 25 MPa to 120 MPa. From figure 3b, the increase in the yield stress of the oxide film material reduces the PEEQ of the base alloy in the crack tip area. The maximum strain value is at θ=0 °on the stress corrosion crack tip passivation circle. The strain changes with θ in three stages and its changing tendency is consistent with stress.

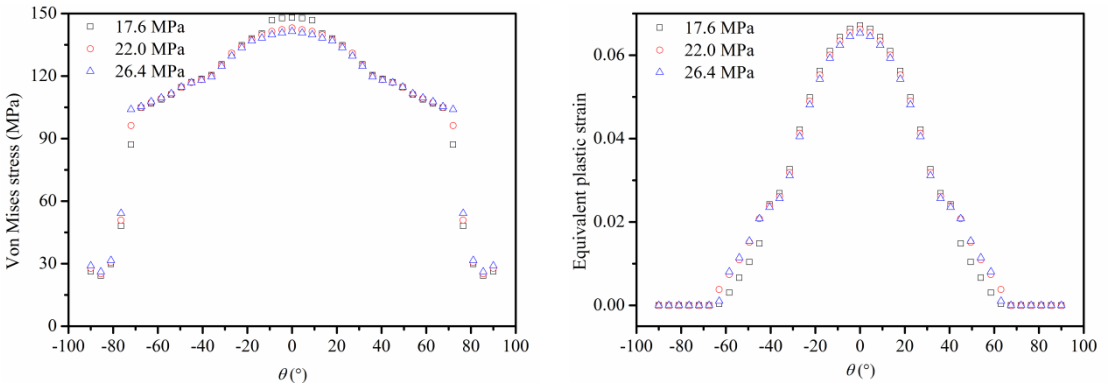

Figure 3. The Mises stress (a) and equivalent plastic strain (b) curve of the base alloy in the crack tip area under the different oxide film material's yield strength.

3.2. Influence of Oxide Film's Yield Stress on the Stress and Strain Along Line 2

Figure 4 is the Mises stress and equivalent plastic strain curve of the oxide film in the crack tip area under the different oxide film material's yield strength. From figure 4a, it can be seen that as the yield strength of oxide film material increases, its Mises stress increases, but the angle of reaching the maximum stress decreases, being 48 °, 40 °, and 36 °, repectively. From figure 4b, as the yield strength of the oxide film material increases, the plastic strain in the oxide film area decreases. The plastic strain is the largest at θ=0 °on the passivation circle of the stress corrosion crack tip. Furthermore, comparing figure 4a and figure 4b, the yield stress of the oxide film material has a greater influence on the stress of the oxide film in the crack tip area than the strain.

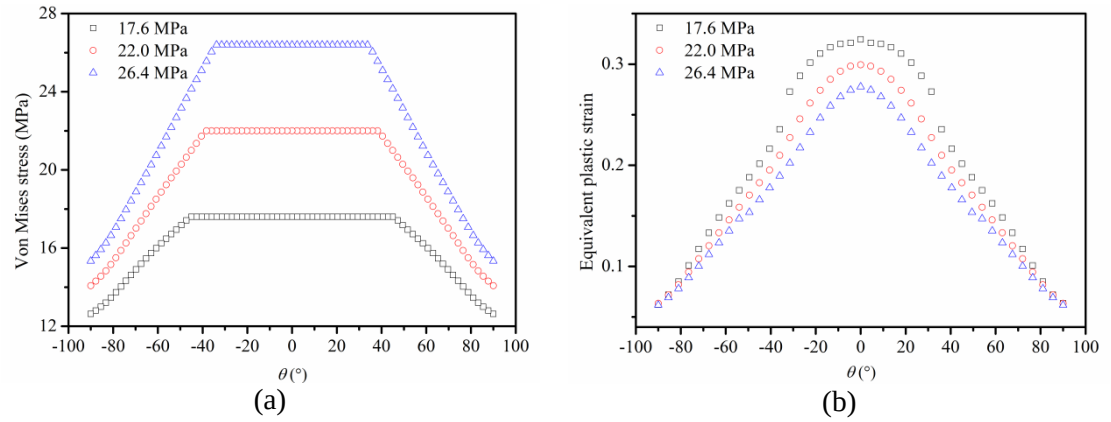

Figure 4. The Mises stress (a) and equivalent plastic strain (b) curve of the oxide film in the crack tip area under the different oxide film material's yield strength.

Comparing figure 3 and figure 4, we can see that the change of the oxide film material has a greater impact on its stress and strain than on the matrix alloy. In addition, it also can be found that as the yield stress of oxide film increases, the stress and strain of base alloy in crack tip area both decrease, and the stress of oxide film in crack tip also reduces, but the strain increases. This is because the oxide film bears more load, so the load on the base alloy of the crack tip becomes smaller, resulting in a reduction in the stress and strain on the base.

3.3. Influence of Oxide Film's Yield Stress on the Stress and Strain along Line 3

Figure 5 shows the stress and strain curve of the crack tip along the crack propagation direction (horizontal direction, observation line 3). From figure 5a, as the distance from the crack tip increases,

the Mises stress in the crack tip area gradually decreases in the oxide film, a sudden change occurs at the boundary between the oxide film and the matrix alloy, and the stress decreases after an instant increase. Moreover, with the yield stress of the oxide film increasing, the stress in the oxide film region increases while the stress in the matrix decreases. From figure 5b, as the distance from the crack tip increases, the PEEQ of the crack tip area decreases. In the oxide film, as the distance increases, the equivalent plastic strain approaches 0.1, and there is no mutation at the boundary between the oxide film and the substrate. In the base metal, as the distance increases, the equivalent strain decreases linearly.

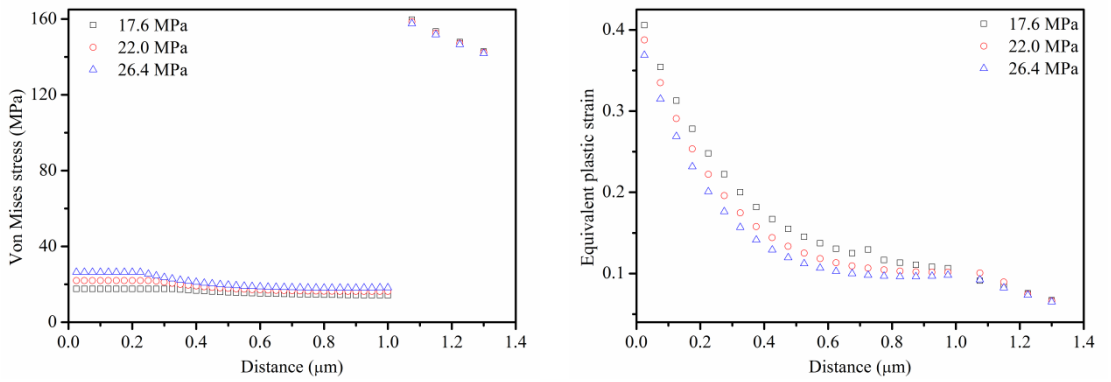

Figure 5. The Mises stress (a) and equivalent plastic strain (b) curve of the crack tip along the crack.

4. Conclusions

In this study, a two-dimensional finite element method is proposed to investigate the fracture parameter in the tip region of SCC of AA6082 alloy. The important conclusions are as follows, the change of the oxide film material has a greater impact on its stress and strain than on the matrix alloy. In addition, it also can be found that as the yield strength of oxide film increases, the stress and strain of base alloy in crack tip area both decrease, and the stress of oxide film in crack tip also reduces, but the strain increases.

Acknowledgment

This work is supported by the Technical Innovation Projects (Project Number 21SG-13) and Shanghai Science and Technology Plan Program (20PJ1417200).

References

[1] Frank R E and J.A. Hawk J A 1989 *Scr. Metall.* **23** 113
[2] Skinner D J, Bye R L, Raybould D and Brown A M 1986 *Scr. Metall.* **20** 867
[3] Sun S B, Zheng L J, Liu Y Y, Liu J H and Zhang H 2015 *Int. Adv. Manuf. Technol.* **80** 1787
[4] Song J, Li X J, Shi S P, Yan L M, Jiang T and Peng S M 2017 *Electrchim. Acta* **248** 4626
[5] Grażyna M N and Sieniawski J 2005 *J. Mater. Process. Tech.* **162** 367
[6] Choi B H, Chudnovsky A and Sehanobish K 2007 *Int. J. Fracture* **145** 81
[7] Fujii T. Tohgo K, Kenmochi A and Shimamura Y 2015 *Corros. Sci.* **97** 139
[8] Nguyen T T, Bolivar J and Réthoré J 2017 *Int. J. Solids Struct.* **112** 65
[9] Zhang Y, Song J, Yan L M, Shi S P and Peng S M 2019 *Electrchim. Acta* **239** 446
[10] Terachi T, Fujii K and Arioka K 2005 *J. Nucl. Sci. Technol.* **42** 225
[11] Kamaya M 2016 *Int. J. Pres. and Pip.* **137** 1